

## Solar and Solar System

### An Improved Oblateness for the Earth's Thermosphere from Lunar Eclipse Observations

Byron W. Soulsby, 32 Greenglade Drive, Paradise, South Australia 5075

**Abstract:** The current ephemerides include an allowance for umbral oblateness based on the flattening of the Earth's geodetic reference spheroid; there are few published estimates for umbral oblateness derived directly from the geometry of a lunar eclipse. This paper reports umbral oblateness values which have been derived from 7,400 crater contact timing observations of twenty-one lunar eclipses by amateur and professional astronomers since 1972. The observed umbral oblateness was found to be typically three times the geodetic reference spheroid flattening.

#### 1. Introduction

Inspired by earlier work in the study of lunar eclipses, particularly the timing of crater extinction by other analysts (Link 1969; Ashbrook 1964, 1977), a suite of 'BASIC' computer programs was developed (Soulsby 1990) to conduct new analyses of eclipse data accumulated over the past two decades. Lunar eclipse circumstances, crater timing predictions and umbral primary contacts were issued to participating astronomers in an Observers' Guide before each eclipse to obtain suitable crater timings for analysis.

#### 2. Method

Computed timing predictions were provided for selected craters using the standard oblateness value for the flattening of the thermosphere of the Earth. Observations were made during lunar eclipses, and the time that each side of a crater made contact with the edge of the umbra during both the immersion and emersion phase was recorded, as illustrated in Figure 1. The resulting 7400 crater contact timings made by more than 200 astronomers were collated for twenty-one lunar eclipses over the period January 1972 to December 1991. The data were analysed by an original method (Soulsby 1984, 1990), using Besselian element coordinates of the Moon and selected craters relative to the umbra centre as origin, to determine the observed umbral geometry for each lunar eclipse. The data include the theoretical and observed radii for each crater contact and the position angles on the umbra edge.

The umbral enlargement (E%) was computed for all crater timings to find the theoretical and observed radii, and the position angle of each lunar feature at the time of contact with the umbral edge. Data within a statistical range of  $0 < E < 4$ , or two standard deviations, were used for the umbral oblateness estimates.

The data for the observed oblateness was accepted where

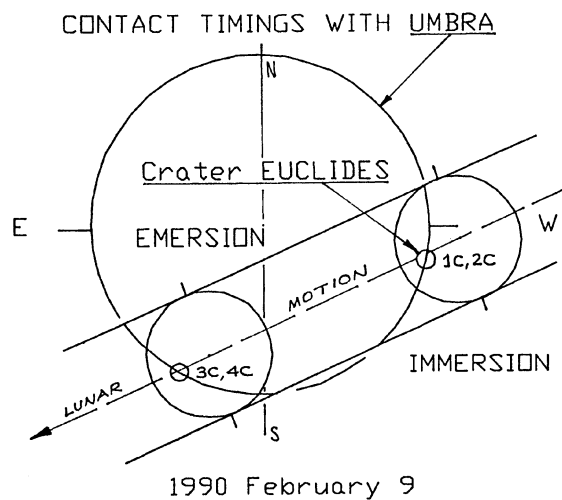


Figure 1 — Crater timing method for the determination of umbral oblateness during a typical lunar eclipse.

the error of the mean was less than 0.15 in E%. Best-fit-ellipse and linear-regression analysis techniques were used to determine the mean values for the polar and equatorial umbral radii,  $R(p)$  and  $R(e)$ , in units of the Earth's radius (this also gives the height of the thermosphere at the pole and equator); the oblateness or flattening is then found from  $[R(e) - R(p)]/R(e)$ . The oblateness is often characterised by the reciprocal of this value.

The umbral radii are highly dependent on the chosen value of oblateness, the position angle of the crater and the circumstances or geometry of the eclipse as shown in Figure 2; here the variations in umbral radius for three possible values of reciprocal oblateness, namely the mean observed (102), the geometric value (214) and the geodetic value (298), are illustrated by the emersion umbral radii ( $R_1$ ,  $R_2$  and  $R_3$ ) and the immersion radii ( $R_5$ ,  $R_6$ ) for the total lunar eclipse of 1990 February 9.

Figure 2 also illustrates that in this case there is very little difference in the radii at immersion for the three possible umbral oblateness values, whereas radii at emersion vary considerably due to the position angle or lunar latitude of the crater. This geometry is considered for each eclipse when determining the umbral oblateness. The eclipse illustrated yielded mean reciprocal oblateness values of 51 from crater immersions and 160 from emersions. This particular eclipse provided adequate data for deriving umbral enlargement from crater immersion and emersion contact timing values and contributed to the data used to compute the mean oblateness.

#### 3. Discussion

The individual reciprocal oblateness values,  $F$ , for each eclipse, are listed in Table 1. There is a large scatter and the mean value is 102. The values are consistently smaller than that of the Earth's Geodetic Reference Spheroid, taken as 298.257 for the reciprocal of flattening (1992, *Astronomical Almanac*, K13), and are smaller than that expected from the geometry of the eclipse which is around 214 (Meeus 1979), which includes atmospheric flattening of 10 km at the pole and equator. In terms of the flattening or oblateness, the mean value for the umbra of  $1/102$  is approximately three times the geodetic value of  $1/298$ .

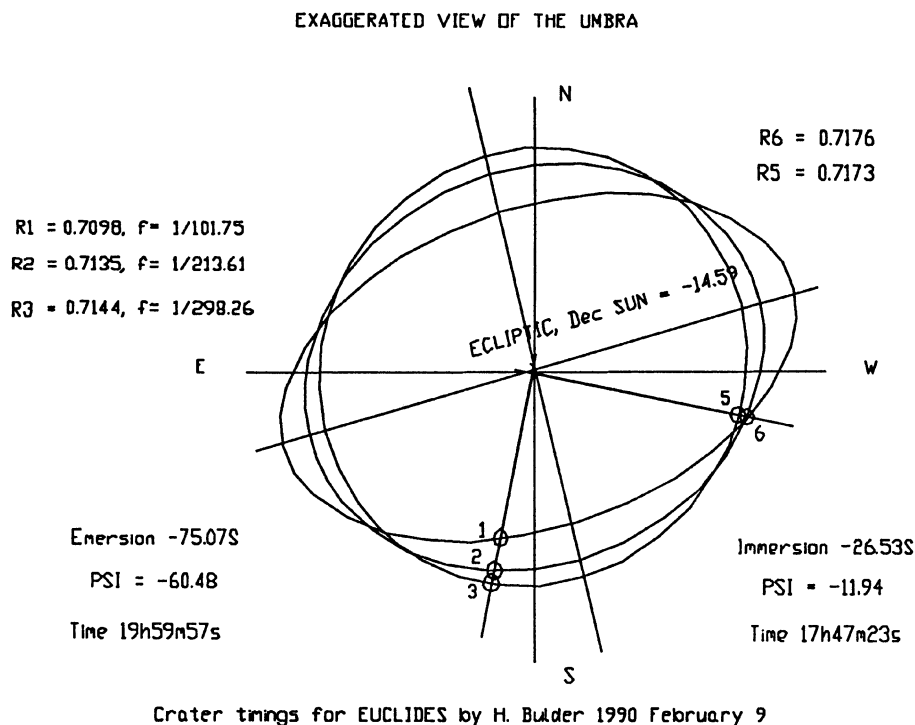


Figure 2 — The theoretical and observed umbral radii dependence on three values of oblateness of the umbra and the geometry of a lunar eclipse. Data contributed by Henk Bulder's observations in the Netherlands of the 1990 February 9 lunar eclipse.

Table 1. Lunar Eclipse Data: reciprocal flattening (F) as a function of Julian Day and true geocentric distance

Date	N/S	JD + 2440000	TGD (AU)	Min F	Max F	Mean F (Imm)	Mean F (Em)
74NOV29	N	2381.43	0.98638	65	132	99	
78MAR24	S	3592.18	0.99692	23	146	124	47
78SEP16	N	3768.30	1.00538	17	206	72	83
79MAR13	N	3946.38	0.99379			158	
79SEP6	S	4123.95	1.00805			138	91
82JAN9	S	4979.33	0.98334	40	98	67	
82JUL6	S	5156.81	1.01667			None	50
82DEC30	S	5333.98	0.98330			None	
83JUN25	S	5510.85	1.01641	41	283	144	68
85MAY4	N	6190.33	1.00832	85	187	149	127
85OCT28	S	6367.24	0.99351			133	
86APR24	S	6545.03	1.00566	16	237	85	119
86OCT17	N	6721.31	0.99661	13	403	115	116
88AUG27	S	7224.96	1.01028			None	133
89FEB20	N	7578.15	0.98876			70#	
89AUG17	S	7755.63	1.01237	39	219	110	
90FEB9	S	7932.30	0.98655	15	430	50	222
90AUG6	N	8110.09	1.01427			None	26
91DEC21	N	8611.94	0.98375			40	40*

#This value is supported by image analysis of CCD video records.

\*Determined by image analysis of CCD video records.

The individual values of reciprocal oblateness in Table 1 show no clear trends as a function of Julian Day. Further investigation was made to see if there is any systematic dependence on true geocentric distance (also given in Table 1). Again, no systematic trends can be seen above the scatter.

It has not been possible to consider atmospheric effects (cloud, volcanic dust, etc) in the hemisphere in which the eclipse is visible. However some of the scatter could be due to these effects rather than measurement errors.

#### 4. Conclusions

The method provides empirical mean values of umbral enlargement and oblateness which have been included as new constants in an improved lunar eclipse ephemeris

(Soulsby 1990) for the prediction of lunar eclipse circumstances and umbral primary and crater contact times.

Current work (Soulsby 1992) applies image analysis techniques to video recordings of recent eclipses to supplement the crater timing data from the 1989 February 20, 1990 February 9 and 1991 December 21 eclipses. In this work it is planned to look for any variation in oblateness with time for each eclipse.

Ashbrook, J., 1977, *Sky and Telescope*, **53**, 173.

Ashbrook, J., 1964, *Sky and Telescope*, **27**, 156.

Link, F., 1969, *Eclipse Phenomena in Astronomy*, Springer-Verlag, Berlin.

Meeus, J., *Sky and Telescope*, 1979, **57**, 333.

Soulsby, B.W., 1986, *Aust. J. Astron.*, **1**, 157.

Soulsby, B.W., 1990, *Aust. J. Astron.*, **3**, 156.

Soulsby, B.W., 1992, *Aust. J. Astron.*, **4**, 143.

Soulsby, B.W., 1984, *J. Brit. Astron. Assoc.*, **95**, 16.

Soulsby, B.W., 1990, *J. Brit. Astron. Assoc.*, **100**, 6.